Use of deep learning-accelerated T2 TSE for prostate MRI: Comparison with and without hyoscine butylbromide admission

M. Boschheidgen, L. Drewes, B. Valentin, T. Ullrich, S. Trappe, R. Al-Monajjed, J.P. Radtke, P. Albers, H.J. Wittsack, G. Antoch, L. Schimmöller

Article - Version of Record

Magnetic Resonance Imaging 118 (2025) 110358

Contents lists available at ScienceDirect

Magnetic Resonance Imaging

journal homepage: www.elsevier.com/locate/mri

Use of deep learning-accelerated T2 TSE for prostate MRI: Comparison with and without hyoscine butylbromide admission

M. Boschheidgen [a], L. Drewes [a], B. Valentin [a], T. Ullrich [a], S. Trappe [a], R. Al-Monajjed [b], J.P. Radtke [b], P. Albers [b], H.J. Wittsack [a], G. Antoch [a,c], L. Schimmöller [a,d,*]

[a] Department of Diagnostic and Interventional Radiology, Univ Dusseldorf, Medical Faculty, Moorenstr. 5, D-40225 Dusseldorf, Germany
[b] Department of Urology, Univ Dusseldorf, Medical Faculty, Moorenstr. 5, D-40225 Dusseldorf, Germany
[c] Center for Integrated Oncology Aachen Bonn Cologne Düsseldorf, Düsseldorf, (CIO ABCD), Germany
[d] Department of Diagnostic, Interventional Radiology and Nuclear Medicine, Marien Hospital Herne, University Hospital of the Ruhr-University Bochum, Herne, Germany

ARTICLE INFO

Keywords:
Multiparametric magnetic resonance imaging
Artificial intelligence
Prostate cancer

ABSTRACT

Objective: To investigate the use of deep learning (DL) T2-weighted turbo spin echo (TSE) imaging sequence with deep learning acceleration (T2DL) in prostate MRI regarding the necessity of hyoscine butylbromide (HBB) administration for high image quality.

Methods: One hundred twenty consecutive patients divided into four groups (30 for each group) were included in this study. All patients received a T2DL (version 2022/23) and a conventional T2 TSE (cT2) sequence on an implemented 3 T scanner and software system. Group A received cT2 with HBB compared to T2DL without HBB with a field of view (FOV) of 130 mm and group B with a FOV of 160 mm. Group C received both sequences with a FOV of 160 mm plus HBB and group D without HBB. Two radiologists independently evaluated all imaging datasets in a blinded reading regarding motion, sharpness, noise, and diagnostic confidence. Furthermore, we analyzed quantitative parameters by calculating edge rise distance (ERD), signal-to-noise-ratio (SNR), and contrast-to-noise-ratio (CNR). Friedman test was used for group comparisons.

Results: Baseline characteristics showed no significant differences between groups A-D. After HBB cT2 showed less motion artifacts, more sharpness, and a higher diagnostic confidence than T2DL, though DL sequences had significantly lower noise ($p < 0.01$). Quantitative analysis revealed higher SNR and CNR for T2DL sequences ($p < 0.01$), while edge rise distance (ERD) remained similar. Inter-reader agreement was good to excellent, with ICCs ranging from 0.84 to 0.93. T2DL acquisition time was significantly lower than for cT2.

Conclusions: In our study, cT2 sequences with HBB showed superior image quality and diagnostic confidence while the T2DL sequence offer promising potential for reducing MRI acquisition times and performed better in quantitative measures like SNR and CNR. Additional studies are required to evaluate further adjusted and developed DL applications for prostate MRI on upcoming scanner generations and to assess tumor detection rates.

Abbreviations: PC, Prostate cancer; DL, Deep Learning; mpMRI, Multiparametric magnetic resonance imaging; EAU, European Association of Urology; PSA, Prostate specific antigen; PSAD, Prostate specific antigen density; DCE, Dynamic contrast enhancement; DWI, Diffusion weighted imaging; PI-RADS, Prostate Imaging and Reporting Archiving Data System; SNR, Signal-to-noise-ratio; CNR, Contrast-to-noise-ratio; FOV, Field of view; ERD, Edge rise distance; TSE, Turbo spin echo; HBB, Hyoscine butylbromide.

* Corresponding author at: Department of Diagnostic and Interventional Radiology, Univ Dusseldorf, Medical Faculty, Moorenstr. 5, D-40225 Dusseldorf, Germany
E-mail addresses: matthias.boschheidgen@med.uni-duesseldorf.de (M. Boschheidgen), LukasRichard.drewes@med.uni-duesseldorf.de (L. Drewes), Birte.valentin@med.uni-duesseldorf.de (B. Valentin), tim.ullrich@med.uni-duesseldorf.de (T. Ullrich), Samuel.trappe@med.uni-duesseldorf.de (S. Trappe), Rouvier.al-monajjed@med.uni-duesseldorf.de (R. Al-Monajjed), JanPhilipp.radtke@med.uni-duesseldorf.de (J.P. Radtke), Peter.Albers@med.uni-duesseldorf.de (P. Albers), hans-joerg.wittsack@med.uni-duesseldorf.de (H.J. Wittsack), Antoch@med.uni-duesseldorf.de (G. Antoch), Lars.Schimmoeller@med.uni-duesseldorf.de (L. Schimmöller).

https://doi.org/10.1016/j.mri.2025.110358
Received 26 January 2025; Received in revised form 8 February 2025; Accepted 8 February 2025
Available online 10 February 2025

1. Introduction

In the detection and classification of prostate cancer (PC), multiparametric magnetic resonance imaging (mp-MRI) of the prostate plays a crucial role in diagnostics [1–4]. Several studies indicate that mpMRI identifies more than 90 % of csPCa cases, reinforcing its role in targeted biopsy strategies [5]. MpMRI includes a combination of anatomical T2-weighted imaging in different orientations and two functional MRI sequences: diffusion-weighted imaging (DWI) and dynamic contrast-enhanced imaging (DCE). These sequences facilitate a standardized evaluation process, adhering to the well-established Prostate Imaging Reporting and Data System (PIRADS v2.1) guidelines [6]. T2-weighted imaging (T2w) should be performed in axial, coronal, and sagittal planes with high spatial resolution, utilizing TSE sequences and a maximum slice thickness of 3 mm without gaps. This results in long examination times and makes diagnosis more difficult as it increases the risk of movement artifacts and insufficient image quality. Short examination times are of fundamental importance if MRI is to be widely used, for example for indications in screening on a populational level [7–11]. There are promising approaches to make T2w- sequences faster and endeavours to shorten the protocols in general [12,13]. The introduction of novel deep learning (DL) reconstruction methods shows promise in reducing examination times while maintaining high image quality and reducing motion artifacts [14,15].

Administration of an anti-peristaltic drug prior to the examination helps to reduce motion-related artifacts due to movement in surrounding structures such as the bladder, rectum, and intestines, which can otherwise impair image quality and diagnostic accuracy [16]. Typically, hyoscine-N-butyl-bromide (also known as hyoscine butylbromide, HBB, scopolamine butylbromide, butylscopolamine) or glucagon are used for this purpose. The use of anti-peristaltic medication is recommended by several studies and is considered potentially beneficial according to the joint guidelines of the European Society of Urogenital Radiology (ESUR), the American College of Radiology (ACR), and the AdMeTech Foundation (PI-RADS Prostate Imaging – Reporting and Data System: 2015, Version 2; PI-RADS v2) [6,17]. However, the disadvantages of the application must also be considered, in particular the risk of an allergic reaction. There are also certain contraindications that make the administration of HBB impossible, such as cardiac arrhythmia or an increase in intraocular pressure [18].

Therefore, the aim of this prospective study was to analyze whether the novel deep learning-accelerated T2 TSE sequence (T2DL) makes the administration of HBB superfluous due to its ability to reduce motion artifacts. We compared the new technique without anti-peristaltic drug to conventional T2 TSE sequences (cT2) in terms of qualitative and quantitative imaging parameters.

2. Materials and methods

2.1. Study design and sample

This prospective study was approved by the local institutional review board and written informed consent was obtained from all subjects. A total of 120 patients from February to October 2023 were included into the study and divided into four different groups. The group size of 30 participants was based on the assumption that statistical differences between the groups could be detected in this way. Exclusion criteria were glaucoma, cardiac arrhythmia and/or ischemic heart disease, myasthenia gravis, known allergy against HBB, and active participation in public traffic (e.g. drivers). All participants were divided into four different groups. Group A received a T2 DL sequence with a FOV of 130 mm followed by a HBB and a conventional T2 TSE with a FOV of 130 mm. In group B, both sequences were acquired with a FOV of 160 mm. Group C compared the FOV 160 mm, whereby both sequences were measured after prior HBB application. Group D received the FOV 160 mm without HBB. For groups A-C, 40 mg of HBB (Buscopan®; Boehringer, Ingelheim, Germany) were administered intravenously according to the manufacturer's protocol. Group A and B received the pharmaceutical on the MRI table. We conducted the second axial T2-weighted TSE- sequence after HBB administration according to the pharmacokinetic profile with a plasma half-life of HBB ($t½\alpha = 4$ min).

The primary objective of the study was to determine, if T2DL sequences without HBB provides the same diagnostic accuracy compared to standard sequences with HBB injection. Secondary objectives were comparison of FOV 130 mm to FOV 160 mm and the effect of HBB in terms of qualitative and quantitative image quality.

2.2. MRI imaging

The MR imaging was conducted on 3 Tesla systems (MAGNETOM Prisma, Software version VE11C) using either a 60-channel phased-array surface coil. The imaging protocol followed PI-RADS v2.1 guidelines, including T2-weighted sequences in three orthogonal planes (axial measurements: 0.5 mm × 0.5 mm × 3.0 mm, field of view of 130 mm), diffusion sequences (utilizing both z-EPI and rs-EPI methodologies), and dynamic contrast sequences. Additionally, T2DL sequence (version 2022/23) was acquired in axial orientation. All technical details regarding the acquired T2-weighted sequences can be found in Table 1. The method is a DL based k-space to image space reconstruction (marketing name: Deep Resolve Boost). The technical details have been described previously [15,19]. An unrolled variational network was utilized for reconstruction. This trainable network alternated between data consistency steps and image regularization steps through a convolutional network. The network input comprised under sampled k-space data, coil sensitivity maps estimated from reference lines, and a normalization field for image homogenization. The reconstruction focused on enhancing the SNR without altering image contrast, ensuring that acquisition parameters like echo time, repetition time, and echo train length remained consistent with conventional reconstructions. Model parameters were determined through supervised training with approximately 10,000 slices from volunteer TSE acquisitions on various clinical 1.5 T and 3 T scanners. The loss function included an L1-norm and a multiscale version of the structural similarity index (SSIM) between network predictions and ground truth images.

2.3. Image interpretation and data analysis

Two experienced radiologists (L.S. and M.B.), each with substantial tenure in prostate MRI interpretation (13 years and 6 years of reading mpMRI, respectively), reviewed the imaging datasets independently. Both readers were blinded to the sequence types. Prostate dimensions were ascertained using volumetric software (DynaCAD, Philips Healthcare), which also informed the calculation of PSAD by correlating serum PSA with prostate volume.

2.4. Qualitative analysis

The assessed categories included:

Table 1
Technical parameter.

	cT2 FOV 130	cT2 FOV 160	T2DL FOV 130	T2DL FOV 160
TE	102	101	102	96
TR	3990	4060	3990	4240
averages	3	2	2	1
Resolution	0.5 × 0.5 × 3.0	0.5 × 0.5 × 3.0	0.5 × 0.5 × 3.0	0.5 × 0.5 × 3.0
SD	3	3	3	3
Matrix	256 × 256	320 × 320	256 × 256	320 × 320
Acquisition time	5:02	4:40	2:48	3:22

- **Motion**: presence of motion artifacts due to bowel or bladder movement.
- **Sharpness**: clarity of prostate boundaries and lesions to periprostatic fat and surroundig tissue, capsule delineation
- **Noise**: presence of overall image noise in the different sequences, blurriness,
- **Diagnostic confidence**: overall impression of the image quality and confidence in PI-RADS scoring.

A five-point Likert scale was used to rate each category, and the results from both radiologists were averaged. A detailed description of the qualitative parameters is provided in supplementary Table 1 (Sup. Table 1).

2.5. Quantitative image analysis

Quantitative analysis involved calculating the apparent SNR and the apparent CNR. The SNR was determined by dividing the signal intensity in the whole prostate by the standard deviation (SD) of the bladder. The CNR was calculated by subtracting the signal intensity of the bladder from the signal intensity of the whole prostate and then dividing by the SD of the bladder. ERD was also measured as an indicator of image sharpness. This was derived from the signal intensity profile of a line drawn across the dorsal prostate capsule. The ERD was defined as the distance between the 10 % and 90 % signal intensity levels relative to the low- and high-signal intensity areas. A shorter ERD indicates sharper delineation of the transition between capsule and fat tissue. The signal intensity values were averaged within equal-sized regions of interest (25 mm^2) in the bladder.

2.6. Statistical analysis

Statistics were performed using IBM SPSS® Statistics (Version 29, IBM Corp). *P*-values <0.05 were defined as statistically significant. Wilcoxon signed rank test was performed to compare continuous data; chi square test was performed to compare categorical data.

3. Results

3.1. Study population

A total of 120 participants with a median age of 64 years (interquartile range (IQR) 57–70 years) were included in this study ranging from 34 to 85 years. The median prostate specific antigen (PSA) was 6,1 ng/ml (IQR 4.5–9.2). 56 patients exhibited prostate volume below 50 ml while 16 had massively enlarged prostates with volumes above 100 ml. PSA- levels, PSAD and PI-RADS scores are shown in Table 2. 52 patients had a PI-RADS score of 4 or 5 and were therefore suspected of having PC. The extent to which a carcinoma was present was not part of the analysis. When comparing the different groups with their respective sequences, there was no significant difference in terms of the clinical data.

3.2. Qualitative imaging parameters

For the HBB effect, the qualitative parameters showed a superiority of the conventional T2 sequence after HBB application compared to the DL sequence regarding image sharpness, motion artifacts and diagnostic confidence, while the noise in the accelerated sequence was significantly lower ($p < 0.01$) (Table 3). This observation applies to both the large FOV and the FOV 130 mm. In the DL accelerated sequence without HBB, the image quality was poor in four cases in the FOV 130 and in three cases in the FOV 160 that there was a score of 2 for diagnostic accuracy. For the conventional T2-sequence, all examinations showed at least moderate diagnostic quality with a score of 3 or higher. A comparison of the conventional T2 sequence with the DL-accelerated sequence without HBB effect showed similar results for both readers (Table 3). With HBB administration, both readers evaluated the T2 sequence better than the DL sequence in terms of diagnostic value (4.64 vs. 3.9; $p < 0.01$). The same observation could be made for the comparison without prior HBB before acquiring the two sequences (4.47 vs. 3.74; $p < 0.01$). The extent of movement artifacts was also lower for groups C and D in the conventional T2 sequence than in the T2 DL sequence (0.9 vs. 2.0 and 1.32 vs. 2.1 respectively; $p < 0.01$) (See Figs. 1-4).

3.3. Quantitative imaging parameters

Considering quantitative imaging parameters, DL showed significantly higher SNR (prostate) and CNR than T2 for all compared groups ($p < 0.01$) (Table 4). The ERD did not differ significantly between both sequences for all comparisons.

3.4. FOV and HBB effect

In the qualitative analysis between FOV 130 and FOV 160 the T2 with FOV 130 and HBB demonstrated fewer motion artifacts than the T2 with FOV 160 and HBB (0.47 vs. 0.77; $p = 0.011$) while the other qualitative parameters showed no statistically significant difference.

Considering the effect of HBB administration on image quality, we could observe a significant reduction in motion artifacts for T2 with FOV160 and HBB compared to T2 with FOV160 and without HBB (0.90 vs. 1.32; $p = 0.027$). Again, other qualitative parameters failed to reach clinical significance.

Table 2
Clinical and MRI parameters.

		All patients	Group A FOV 130 +/−	Group B FOV 160 +/−	Group C FOV 160 +	Group D FOV 160 -
Patients (n)		120	30	30	30	30
Age in years;		64	66	63	63	66
median (IQR)		(57–70)	(57–74)	(57–70)	(57–68)	(57–70)
Prostate Volume in ml;		52	53	48	57.5	51
Median (IQR)		(36–77)	(37–73)	(33–85)	(35–77)	(37–77)
PSA in ng/ml;		6.1	6.3	5.3	6.1	7.2
median (IQR)		(4.5–9.2)	(4.5–8.7)	(3.7–7.8)	(4.5–9.9)	(5.1–10.7)
PSAD		0.12	0.14	0.09	0.12	0.13
median (IQR)		(0.08–0.17)	(0.07–0.18)	(0.07–0.13)	(0.09–0.18)	(0.11–0.19)
	1	0	0	0	0	0
	2	35	8	12	6	9
PI-RADS v2.1 (n)	3	33	7	7	8	11
	4	37	10	7	12	8
	5	15	5	4	4	2

PSA = prostate specific antigen; PSAD = prostate specific antigen density; IQR = interquartile range.

Table 3
Qualitative imaging Parameters.

	Group A FOV 130 +/−			Group B FOV 160 +/−			Group C FOV 160 +			Group D FOV 160 -			
	cT2 +	T2DL -	P	cT2 +	T2DL -	P	cT2 +	T2DL +	P	cT2 -	T2DL -	p	
Patients (n)	30			30			30			30			
Motion Mean (SD)	0.47 (±0.72)	2.17 (±0.85)	**<0.01**	0.77 (±0.79)	1.67 (±0.90)	**<0.01**	0.9 (±1.02)	2.0 (±0.84)	**<0.01**	1.32 (±1.10)	2.1 (±0.80)	**<0.01**	
Sharpness Mean (SD)	4.57 (±0.59)	3.03 (±0.61)	**<0.01**	4.32 (±0.72)	3.50 (±0.70)	**<0.01**	4.5 (±0.60)	3.48 (±0.72)	**<0.01**	4.23 (±0.79)	3.5 (±0.70)	**<0.01**	
Noise Mean (SD)	2.18 (±0.65)	1.03 (±0.32)	**<0.01**	1.78 (±0.61)	0.97 (±0.41)	**<0.01**	2.47 (±0.79)	1.55 (±0.72)	**<0.01**	2.15 (±0.66)	1.55 (±0.62)		**<0.01**
Diagnostic confidence Mean (SD)	4.75 (±0.44)	3.30 (±0.70)	**<0.01**	4.53 (±0.65)	3.75 (±0.68)	**<0.01**	4.63 (±0.58)	3.9 (±0.82)		**<0.01**	4.47 (±0.75)	3.73 (±0.69)	**<0.01**

FOV = field-of-view in mm; T2 = T2-weighted-sequence; DL = deep learning accelerated T2-weighted sequence.

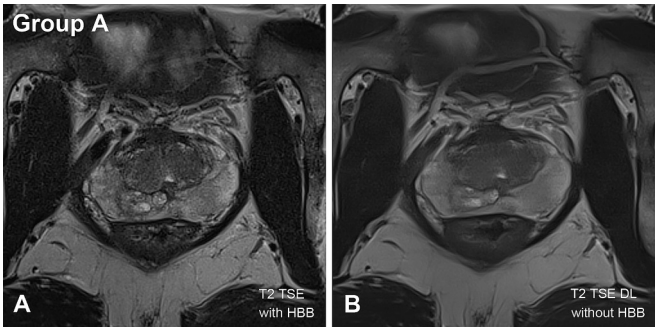

Fig. 1. Example of group A: cT2 with FOV 130 and HBB compared to T2DL with FOV 130 and without HBB.

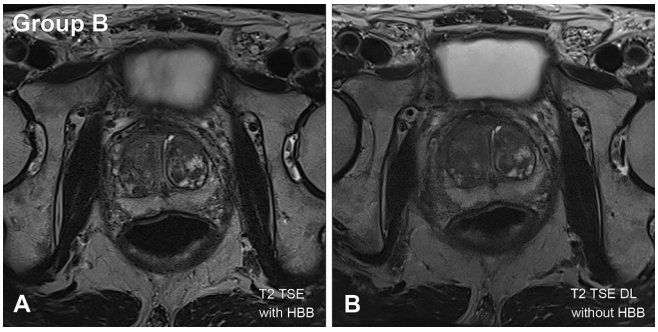

Fig. 2. Example of group B: cT2 with HBB and T2DL without HBB, each with FOV 160.

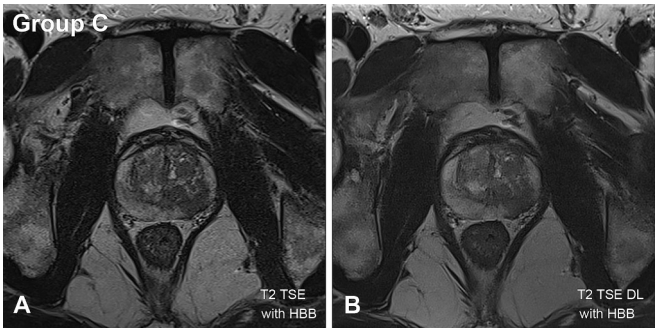

Fig. 3. Example of group C: cT2 and T2DL with FOV 160 and HBB.

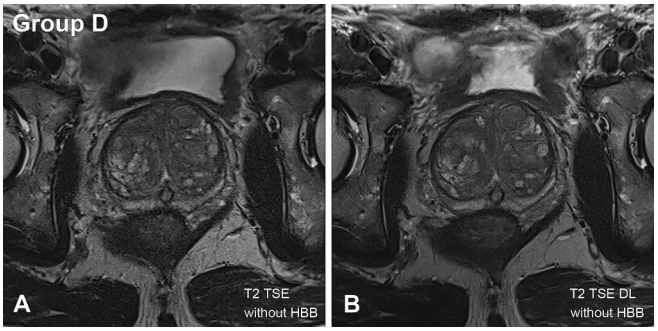

Fig. 4. Example of group D: cT2 and T2DL with FOV 160 without HBB.

3.5. Intraclass correlation

Intraclass correlation coefficients (ICC) between different readers demonstrated good to excellent agreement across all assessed qualitative categories, with values ranging from 0.84 to 0.93. Median qualitative scores and IQRs for ICC are displayed in Table 4 (Table 5).

4. Discussion

Prostate MRI offers a non-invasive way to detect clinically significant PC at an early stage and at the same time reduce the number of unnecessary biopsies for clinically insignificant carcinomas. However, the growing demand is offset by the limiting factor of long examination times. A promising approach is the use of DL-accelerated sequences. These innovative sequences enable image acquisition in less time and also promise better image quality and fewer artifacts. One question regarding DL-accelerated sequences was whether, due to artifact suppression, they make the administration of HBB unnecessary, which is still recommended to suppress intestinal activity in order to optimize the image quality. Our results suggest that HBB is able to improve image quality by reducing motion artifacts and that the T2-DL sequence in version and on the scanner platform used alone do not achieve this artifact reduction at the same level. Clear visualization of the relevant anatomical structures forms the foundation for accurate diagnostics and aids in tumor detection.

Previous studies have shown that DL sequences not only significantly shorten the examination time but can also lead to an improvement in image quality and reduce motion artifacts [14]. Motion artifacts are also reduced by the application of HBB [16].

In this comparative study, we acquired conventional T2 sequences with intravenous HBB application and T2-weighted DL-accelerated sequences without HBB and assessed qualitative and quantitative image parameters. In contrast to previous studies, the conventional T2 sequence proved to be superior to the DL sequence in our study, which

Table 4
Quantitative imaging parameters.

	Group A FOV 130 +/−			Group B FOV 160 +/−			Group C FOV 160 +			Group D FOV 160 -		
	cT2 +	T2DL -	P	cT2 +	T2DL -	P	cT2 +	T2DL +	P	cT2 -	T2DL -	p
Patients (n)	30			30			30			30		
SNR Prostate Mean (SD)	2.16	2.57	**<0.01**	2.22	2.53	**<0.01**	2.21	2.56	**<0.01**	2.18	2.48	**<0.01**
SNR Bladder Mean (SD)	54.62	56.27	0.988	63.28	42.22	**<0.01**	59.53	42.46	**<0.01**	57.41	46.40	**<0.01**
CNR Mean (SD)	0.55	0.83	**<0.01**	0.61	0.98	**<0.01**	0.52	0.91	**<0.01**	0.58	0.95	**<0.01**
ERD Mean (SD)	1.75	1.33	0.438	1.30	1.87	0.164	1.76	1.47	0.068	1.33	1.50	0.53

FOV = field-of-view in mm; T2 = T2-weighted-sequence; DL = deep learning accelerated T2-weighted sequence; SNR = signal-to-noise ratio; CNR = contrast-to-noise ratio; ERD = edge rise distance.

Table 5
Intraclass Correlation between both Readers.

ICC	cT2	T2DL
Motion	0.93	0.87
Median (IQR)	(0.90–0.95)	(0.90–0.91)
Sharpness	0.90	0.86
Median (IQR)	(0.85–0.93)	(0.80–0.90)
Noise	0.85	0.93
Median (IQR)	(0.79–0.90)	(0.90–0.95)
Diagnostic confidence	0.87	0.85
Median (IQR)	(0.81–0.91)	(0.79–0.90)

ICC = intraclass correlation; T2 = T2-weighted-sequence; DL = deep learning accelerated T2-weighted sequence.

underlines the importance of HBB. These results are consistent with the findings of Ullrich et al. and other studies, who demonstrated an improvement in image quality by reducing artifacts and improving anatomical delineation [16,20–22].

Interestingly, our direct comparison between conventional T2 and DL sequences, where both were acquired with or without HBB administration, also showed a superiority of the conventional T2 sequence regarding qualitative parameters, while DL outperformed the conventional T2 in terms of quantitative values as SNR and CNR. These results contradict the studies by Bischoff et al., Oerther et al., and Gassenmeier et al. which showed both a significant shortening of MRI protocols and an improvement in image quality with DL sequences [14,15,23]. The reason for DL sequence being superior regarding quantitative parameters as SNR and CNR is explainable, as these DL sequences rely on optimized image reconstruction methods and data-driven models. First, there is noise reduction through DL algorithms. DL models are particularly adept at identifying and suppressing noise in image data by using information from neighboring pixels and sequences and thereby increase the SNR. Second, DL-based reconstruction methods allow the use of fewer measurement data (reduced acquisition) while reconstructing the image with high quality. Through intelligent interpolation and reconstruction, more detailed images with better CNR can be produced without needing additional measurement data. Many DL algorithms leverage known features of image data (e.g., anatomical structures or typical noise characteristics) from training datasets to improve image reconstruction. Nevertheless, the conventional T2 sequence is superior in the other qualitative parameters except image noise. This is also understandable. By acquiring more image data, the conventional image appears significantly more detailed and sharper. Even the smallest structures can be clearly delineated, whereas the DL image is sometimes washed out and blurry and smaller image details are simply lost. While the softer appearance of the DL sequence led to a reduction in image noise as expected, this was at the expense of image detail, which led to poorer performance in the other qualitative parameters. The high interrater reliability of >0.9 supports the validity of our results. At this point, however, it must also be pointed out that the standard T2 sequence used here has been maximally optimized and had an exceptionally small FOV and therefore offers a very high resolution and good image quality. In contrast, the new DL sequence used was out of the box in development version for a scanner software platform available for some time (VE11C) and has not undergone an optimization process over time/years. A small FOV is generally more sensitive to convolutions. A compromise must be found between acceleration with corresponding SNR loss and sufficient image information. Excessive acceleration can lead to insufficient SNR/image information being measured. This missing information cannot be recovered by DL denoising. Sequence optimization is necessary when using new sequences and they should not simply be used without meticulous adjustments. The extent to which a similar image quality can be achieved through this process should be evaluated on upcoming scanner systems and further improved sequences.

The comparison of groups C and D showed that the movement artifacts were less pronounced in the conventional T2w sequence than in the T2DL. This may seem surprising at first, but there is a simple reason for this. Due to the examination protocol, the T2DL sequence was acquired immediately after HBB administration while cT2 was acquired with some delay. The effect of the HBB seems greater in the later course of the examination and the movement artifacts were less pronounced here. It is therefore not possible to conclusively assess whether the T2DL sequence contains less movement under the same conditions. To answer this question, the protocol would have to be changed, and the sequences analyzed under the same conditions.

DL methods, particularly convolutional neural networks (CNNs), have been widely utilized in prostate mpMRI, primarily for cancer diagnosis [24–26]. Other research areas in prostate MRI include the analysis of tumor aggressiveness [27]. Despite these promising studies highlighting potential DL applications, commercially available products remain limited. As mentioned initially, there is a need to shorten acquisition times due to the high demand for investigations. DL-based approaches offer a very good opportunity here. However, this should not be at the expense of image quality. Our study did not aim to investigate whether the tumor detection rates differ significantly between the different sequences. The differences in diagnostic value do indicate that both readers in the collective analyzed here were more certain regarding their diagnosis in the conventional T2 sequence. However, the extent to which this results in differences in the PI-RADS score or implies other diagnostic steps (biopsy/follow-up) cannot be answered with the design presented here. Further studies are needed to answer that question.

Our study has several limitations. Based on our study design, no conclusions can be drawn about tumor detection. Further studies are required to evaluate the detection of PC using DL sequences. For the evaluation of the HBB effect, we compared two different patient groups either with or without HBB. Considering the wide anatomical

variability, as well as the differing amounts of intraluminal gas and filling, an intra-individual comparison conducted within a single MRI examination in consecutive order would provide a more reliable study design. Finally, the DL sequence used in this study was set in the development stage at the time of the study and on a longtime implemented scanner and software system. Newer further developed sequences and scanner/software generation might perform different. The applied DL is a k-space to image space reconstruction (marketing name: Deep Resolve Boost). Recently, DL based super resolution (Deep Resolve Sharp) is available, which typically increases the image sharpness, especially in cases where the DL reconstruction leads to slightly blurred sharpness. Typically, both algorithms are used in combination. Still, the first publications on TSE DL also used DL without super resolution.

5. Conclusion

Deep learning-accelerated sequences offer promising potential for reducing MRI acquisition times, but in our study, conventional T2 sequences with HBB showed superior image quality and diagnostic confidence compared to DL sequences on the development stage used. While DL sequences performed better in quantitative measures like SNR and CNR, they lacked the detail and sharpness provided by conventional sequences. HBB remains important for reducing motion artifacts and optimizing image quality. Sequence adjustment and optimization is essential when using new (deep learning) sequences. Further development and scanner plus examination specific customization of advanced techniques for upcoming scanner software generations seems very likely improve image quality with simultaneously reduced acquisition time.

CRediT authorship contribution statement

M. Boschheidgen: Writing – original draft, Visualization, Validation, Investigation, Formal analysis, Data curation, Conceptualization. **L. Drewes:** Software, Investigation, Data curation. **B. Valentin:** Writing – review & editing, Resources, Investigation. **T. Ullrich:** Writing – review & editing, Software, Methodology. **S. Trappe:** Writing – review & editing, Visualization, Formal analysis. **R. Al-Monajjed:** Writing – review & editing, Methodology, Investigation, Data curation. **J.P. Radtke:** Writing – review & editing, Validation, Data curation, Conceptualization. **P. Albers:** Writing – review & editing, Validation, Resources. **H.J. Wittsack:** Writing – review & editing, Validation, Methodology, Conceptualization. **G. Antoch:** Writing – review & editing, Supervision, Resources, Conceptualization. **L. Schimmöller:** Writing – review & editing, Visualization, Validation, Supervision, Resources, Project administration, Methodology, Investigation, Formal analysis, Data curation, Conceptualization.

Appendix A. Supplementary data

Supplementary data to this article can be found online at https://doi.org/10.1016/j.mri.2025.110358.

References

[1] Drost F-JH, Osses DF, Nieboer D, et al. Prostate MRI, with or without MRI-targeted biopsy, and systematic biopsy for detecting prostate cancer. Cochrane Database Syst Rev 2019;4(4):CD012663.
[2] van der Leest M, Cornel E, Israël B, et al. Head-to-head comparison of Transrectal ultrasound-guided prostate biopsy versus multiparametric prostate resonance imaging with subsequent magnetic resonance-guided biopsy in biopsy-naïve men with elevated prostate-specific antigen: a large prospective multicenter clinical study. Eur Urol 2019;75(4):570–8.
[3] Rouvière O, Puech P, Renard-Penna R, et al. Use of prostate systematic and targeted biopsy on the basis of multiparametric MRI in biopsy-naive patients (MRI-FIRST): a prospective, multicentre, paired diagnostic study. Lancet Oncol 2019;20(1):100–9.
[4] Ahmed HU, El-Shater Bosaily A, Brown LC, et al. Diagnostic accuracy of multi-parametric MRI and TRUS biopsy in prostate cancer (PROMIS): a paired validating confirmatory study. Lancet 2017;389(10071):815–22.
[5] Pepe P, Garufi A, Priolo GD, Galia A, Fraggetta F, Pennisi M. Is it time to perform only magnetic resonance imaging targeted cores? Our experience with 1,032 men who underwent prostate biopsy. J Urol 2018;200(4):774–8.
[6] Turkbey B, Rosenkrantz AB, Haider MA, et al. Prostate Imaging Reporting and Data System Version 2.1: 2019 Update of prostate imaging reporting and data system version 2. Eur Urol 2019;76(3):340–51.
[7] Auvinen A, Tammela TLJ, Mirtti T, et al. Prostate Cancer screening with PSA, Kallikrein panel, and MRI: the ProScreen randomized trial. JAMA 2024;331(17):1452–9.
[8] Boschheidgen M, Albers P, Schlemmer H-P, et al. Multiparametric magnetic resonance imaging in prostate Cancer screening at the age of 45 years: results from the first screening round of the PROBASE trial. Eur Urol 2024;85(2):105–11.
[9] Hugosson J, Månsson M, Wallström J, et al. Prostate Cancer screening with PSA and MRI followed by targeted biopsy only. N Engl J Med 2022;387(23):2126–37.
[10] Nam R, Patel C, Milot L, et al. Prostate MRI versus PSA screening for prostate cancer detection (the MVP study): a randomised clinical trial. BMJ Open 2022;12(11):e059482.
[11] Nordström T, Discacciati A, Bergman M, et al. Prostate cancer screening using a combination of risk-prediction, MRI, and targeted prostate biopsies (STHLM3-MRI): a prospective, population-based, randomised, open-label, non-inferiority trial. Lancet Oncol 2021;22(9):1240–9.
[12] Kuhl CK, Bruhn R, Krämer N, Nebelung S, Heidenreich A, Schrading S. Abbreviated Biparametric prostate MR imaging in men with elevated prostate-specific antigen. Radiology 2017;285(2):493–505.
[13] Bischoff LM, Katemann C, Isaak A, et al. T2 Turbo spin Echo with compressed sensing and propeller acquisition (sampling k-space by utilizing rotating blades) for fast and motion robust prostate MRI: comparison with conventional acquisition. Invest Radiol 2023;58(3):209–15.
[14] Bischoff LM, Peeters JM, Weinhold L, et al. Deep learning super-resolution reconstruction for fast and motion-robust T2-weighted prostate MRI. Radiology 2023;308(3):e230427.
[15] Gassenmaier S, Afat S, Nickel D, Mostapha M, Herrmann J, Othman AE. Deep learning-accelerated T2-weighted imaging of the prostate: reduction of acquisition time and improvement of image quality. Eur J Radiol 2021;137:109600.
[16] Ullrich T, Quentin M, Schmaltz AK, et al. Hyoscine butylbromide significantly decreases motion artefacts and allows better delineation of anatomic structures in mp-MRI of the prostate. Eur Radiol 2018;28(1):17–23.
[17] Rooij M, Israël B, Tummers M, et al. ESUR/ESUI consensus statements on multi-parametric MRI for the detection of clinically significant prostate cancer: quality requirements for image acquisition, interpretation and radiologists' training. Eur Radiol 2020;30(10):5404–16.
[18] Dyde R, Chapman AH, Gale R, Mackintosh A, Tolan DJM. Precautions to be taken by radiologists and radiographers when prescribing hyoscine-N-butylbromide. Clin Radiol 2008;63(7):739–43.
[19] Hammernik K, Klatzer T, Kobler E, et al. Learning a variational network for reconstruction of accelerated MRI data. Magn Reson Med 2018;79(6):3055–71.
[20] Schmidt C, Hötker AM, Muehlematter UJ, Burger IA, Donati OF, Barth BK. Value of bowel preparation techniques for prostate MRI: a preliminary study. Abdom Radiol (NY) 2021;46(8):4002–13.
[21] Brennan DL, Lazarakis S, Lee A, Tan TH, Chin KY, Oon SF. Do antispasmodics or rectal enemas improve image quality on multiparametric prostate MRI? An 'Evidence-based Practice' review of the literature. Abdom Radiol (NY) 2021;46(6):2770–8.
[22] Wagner M, Rief M, Busch J, et al. Effect of butylscopolamine on image quality in MRI of the prostate. Clin Radiol 2010;65(6):460–4.
[23] Oerther B, Engel H, Nedelcu A, et al. Performance of an ultra-fast deep-learning accelerated MRI screening protocol for prostate cancer compared to a standard multiparametric protocol. Eur Radiol 2024;34(11):7053–62.
[24] Cai JC, Nakai H, Kuanar S, et al. Fully automated deep learning model to detect clinically significant prostate Cancer at MRI. Radiology 2024;312(2):e232635.
[25] Hamm CA, Baumgärtner GL, Biessmann F, et al. Interactive explainable deep learning model informs prostate Cancer diagnosis at MRI. Radiology 2023;307(4):e222276.
[26] Michaely HJ, Aringhieri G, Cioni D, Neri E. Current value of Biparametric prostate MRI with machine-learning or deep-learning in the detection, grading, and characterization of prostate Cancer: a systematic review. Diagnostics (Basel) 2022;12(4).
[27] Cuocolo R, Cipullo MB, Stanzione A, et al. Machine learning applications in prostate cancer magnetic resonance imaging. European Radiology Experimental 2019;3(1).